Nanomaterial safety for microbially-colonized hosts: Microbiota-mediated physisorption interactions and particle-specific toxicity

Brinkmann, B.W.

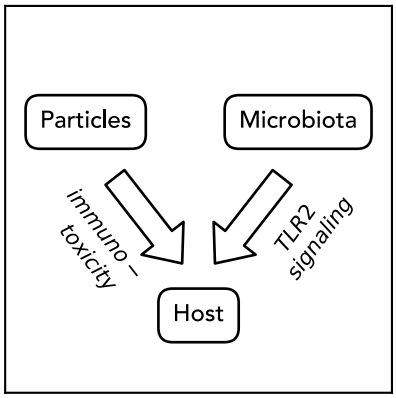
Particles
Microbiota
immuno –
toxicity
TLR2
signaling
Host

CHAPTER 5

Microbiota-dependent TLR2 signaling reduces silver nanoparticle toxicity to zebrafish larvae

Bregje W. Brinkmann

Bjørn E. V. Koch

Willie J. G. M. Peijnenburg

Martina G. Vijver

Published in *Ecotoxicology and Environmental Safety*, 237: 113522 (2022). DOI: 10.1016/j.ecoenv.2022.113522

Data is available via *Mendeley Data*. DOI: 10.17632/4nfg69v8hy.1

Abstract

Many host-microbiota interactions depend on the recognition of microbial constituents by toll-like receptors of the host. The impacts of these interactions on host health can shape the host's response to environmental pollutants such as nanomaterials. Here, we assess the role of toll-like receptor 2 (TLR2) signaling in the protective effects of colonizing microbiota against silver nanoparticle (nAg) toxicity to zebrafish larvae. Zebrafish larvae were exposed to nAg for two days, from 3-5 days post-fertilization. Using an *il1ß*-reporter line, we first characterized the accumulation and particle-specific inflammatory effects of nAg in the total body and intestinal tissues of the larvae. This showed that silver gradually accumulated in both the total body and intestinal tissues, yet specifically caused particle-specific inflammation on the skin of larvae. Subsequently, we assessed the effects of microbiota-dependent TLR2 signaling on nAg toxicity. This was done by comparing the sensitivity of loss-of-function zebrafish mutants for TLR2, and each of the TLR2-adaptor proteins MyD88 and TIRAP (Mal), under germ-free and microbially-colonized conditions. Irrespective of their genotype, microbially-colonized larvae were less sensitive to nAg than their germ-free siblings, supporting the previously identified protective effect of microbiota against nAg toxicity. Under germ-free conditions, *tlr2*, *myd88* and *tirap* mutants were equally sensitive to nAg as their wildtype siblings. However, when colonized by microbiota, *tlr2* and *tirap* mutants were more sensitive to nAg than their wildtype siblings. The sensitivity of microbially-colonized *myd88* mutants did not differ significantly from that of wildtype siblings. These results indicate that the protective effect of colonizing microbiota against nAg-toxicity to zebrafish larvae involves TIRAP-dependent TLR2 signaling. Overall, this supports the conclusion that host-microbiota interactions affect nanomaterial toxicity to zebrafish larvae.

Keywords: Host-microbiota interactions; Toll-like receptor; Zebrafish mutants; Inflammation; IL1ß; NM-300K.

5.1 Introduction

Vertebrate animals depend on their interactions with commensal microbes, residing in and on their tissues, to maintain optimal health. These host-microbiota interactions in, amongst others, immune responses, nutrient uptake and energy metabolism (Hacquard et al. 2015; Brugman et al. 2018), can enhance the resilience of the host to environmental pollutants, including engineered nanoparticles. Microbes have also been shown to directly interact with environmental pollutants, for instance by excreting ligands and other biomacromolecules, by facilitating redox reactions, and by decomposing organic chemicals and coatings (Claus et al. 2016; Desmau et al. 2020). In the case of nanoparticles, this can transform the aggregation state, dissolution rate and surface chemistry of the particles, potentially altering their bioavailability, reactivity, persistence, and toxicity (Lowry et al. 2012). Additionally, nanoparticles can adsorb onto the surface of microbes and microbial spores, forming microbe-particle complexes, which can change the fate and (patho)biological effects of the concerning microbes and particles in relevant, yet largely understudied ways (Westmeier et al. 2018). It is difficult to differentiate between the impacts such microbe-particle interactions, and the effects of host-microbiota interactions when studying nanoparticle toxicity *in vivo*.

Many of the balanced interactions between hosts and commensal microbiota are based on evolutionarily conserved principles, where receptors of the toll-like receptor (TLR) family function to sense microbial cells (Fig. 5.1a). The receptors of this family, which are either located in cell membranes (such as TLR1, -2, -4, -5, -6 and -10) or in intracellular vesicles (like TLR3, -7, -8, -9, -11 and -13), were initially found to detect invading pathogens by sensing common constituents of their cells, termed pathogen-associated molecular patterns (PAMPs), or more generally, microbe-associated molecular patterns (MAMPs). Upon recognition of these ligands, TLR receptors form dimers with intracellularly oligomerized Toll/IL-1 receptor (TIR) domains. Dimerized TLRs subsequently recruit TIR-domain including adaptor proteins such as Myeloid Differentiation factor 88 (MyD88) and Toll/Interleukin-1 Receptor domain-containing Adaptor Protein (TIRAP), also known as MyD88 Adaptor-Like (Mal). The recruitment of these adaptor proteins results in a pro-inflammatory signaling cascade that functions to clear the infection (Li et al. 2017; Hu et al. 2019).

Over the past decade, some TLRs, such as TLR2 (Round et al. 2011; Koch et al. 2018), have also been found to detect MAMPs of commensal microbes. As opposed to host-pathogen interactions, this has been found to dampen pro-inflammatory responses (Koch et al. 2018) (Fig. 5.1a), and has moreover been shown to induce mucin secretion (Birchenough et al. 2016; Paone and Cani 2020), thereby enabling commensal microbes to colonize host tissue without penetrating the mucosal barrier. Theoretically, such immuno-suppressive effects of commensal microbiota could also inhibit the pro-

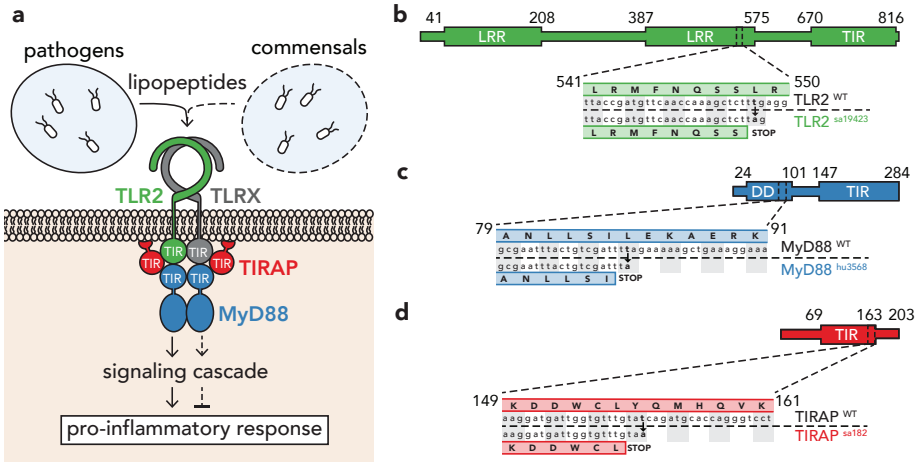

Figure 5.1: *Mutant zebrafish lines in the TLR2 signaling pathway*. **a**) Schematic representation of TLR2 with its adaptor proteins MyD88 and TIRAP (Mal). The Toll/IL-1 receptor (TIR) domain of MyD88 and TIRAP (Mal) can interact with the TIR domain of TLR2. Pathogens have been found to induce pro-inflammatory immune responses via TLR2 (solid line), while commensal microbiota have been shown to dampen pro-inflammatory responses via TLR2 (dashed line). **b**) - **d**) Mutant and wildtype alleles with encoded proteins for TLR2 (*tlr2*^{sa19423} mutant allele) (**b**); MyD88 (*myd88*^{hu3568} mutant allele) (**c**); and TIRAP (Mal) (*tirap*^{sa182} mutant allele) (**d**). In all mutant alleles, a threonine to alanine point mutation results in a premature stop codon prior to or inside of the open reading frame for the TIR domain. As a consequence, the mutants produce truncated versions of TLR2, MyD88 or TIRAP, lacking a functional TIR domain. *Abbreviations*: DD, death domain; LRR, leucine rich repeat; Mal, MyD88 Adaptor-Like; MyD88, Myeloid Differentiation factor 88; TIR, Toll/IL-1 receptor domain; TIRAP, Toll/Interleukin-1 Receptor domain-containing Adaptor Protein; TLR, Toll-Like Receptor.

inflammatory responses of vertebrate hosts to immuno-toxic nanoparticles. Additionally, colonizing microbiota were found to stimulate the proliferation of epithelial cells in the small intestines by enhancing TLR2 expression (Hörmann et al. 2014). As suggested by Hörmann et al. (2014), in addition to potentially beneficial effects of this response to host-microbiota homeostasis, it may explain the protective effects of TLR2 against chemical (DSS)-induced epithelial injury (Rakoff-Nahoum et al. 2004). Similar protective effects of TLR2 signaling can be expected for nanoparticle-induced epithelial injury.

In this study, we investigate the hypothesis that host-microbiota interactions can protect vertebrate hosts against the pro-inflammatory effects of nanoparticles, focusing on the acute toxicity of silver nanoparticles (nAg) to zebrafish larvae. We have previously shown that colonizing microbiota protect zebrafish larvae against the toxicity of these particles (Brinkmann et al. 2020). Moreover, nAg has been shown to induce

acute immuno-toxic adverse effects in both animal models and *in vitro* systems (Poon et al. 2019; Cronin et al. 2020). Here, we aim to deepen our understanding on the marked protection of colonizing microbiota against nAg toxicity to zebrafish larvae, investigating the role of TLR signaling.

To test our hypothesis, we take a threefold approach. Firstly, to characterize nanoparticle exposures, we measured the total accumulation of silver in total and intestinal tissues of exposed larvae. Secondly, to verify the pro-inflammatory effects of the particles, we quantified and localized the particle-specific expression of *il1ß*, encoding the pro-inflammatory cytokine IL1ß, using a fluorescent zebrafish reporter line. Thirdly, to evaluate the role of TLR2 signaling in the protective effect of microbiota against these adverse effects, we compared the sensitivity of three mutants in the TLR2 signaling pathway to that of wildtype siblings under germ-free and microbially-colonized conditions. We focused on a loss-of-function mutant for TLR2, as well as on loss-of-function mutants for the TLR2 adaptor proteins MyD88 and TIRAP. Given the key role of TLR2-signaling in host-microbiota interactions, these efforts help to elucidate the impact of host-microbiota interactions on nAg toxicity to zebrafish larvae. More generally, this work provides a proof-of-principle to discriminate between the effects of microbe-pollutant and host-microbiota interactions on toxicity based on evolutionarily conserved pathways in host-microbiota signaling.

5.2 Methods

5.2.1 Nanoparticle dispersions

Silver nanoparticles (nAg) of series NM300-K (Klein et al. 2011) were kindly provided by HeiQ RAS AG (Regensburg, Germany). Non-dispersed particles were handled in an argon atmosphere to prevent particle oxidation, following the EAHC NANOGENOTOX batch dispersion protocol (v.1) (Jensen 2018b). Particle dispersions were prepared from a 100 mg nAg·L^{-1} stock suspension of nAg in autoclaved egg water (60 mg·L^{-1} Instant Ocean sea salts in demi water; Sera GmbH, Heinsberg, Germany). Stock suspensions were dispersed for 10 min in an ultrasonic bath (USC200T; VWR, Amsterdam, The Netherlands) at an acoustic power of 12W, as determined following the EU FP7 NANoREG sonicator calibration standard operation procedure (v.1.1) (Jensen et al. 2018).

Immediately following dispersion, stock suspensions were diluted to nominal exposure concentrations of 2.5, 1.5, 1.0, 0.75 and 0.25 mg nAg·L^{-1} in autoclaved egg water. As determined in our previous study (Brinkmann et al. 2020), this corresponded to actual concentrations averaging 1.53, 1.49, 0.89, 0.74 and 0.20 mg nAg·L^{-1}, and shed ion concentrations averaging 0.17, 0.09, 0.07, 0.04, and 0.05 mg Ag^{+}·L^{-1}, respectively.

Our previous characterization of the exposure media furthermore indicated that primary particles were spherically shaped, had a mean diameter of 8 to 42 nm (average 24 nm, *n*=50), and formed aggregates with a hydrodynamic size of 140 ± 59 to 218 ± 109 nm at nominal exposure concentrations of 2.5 and 1.5 mg nAg·L^{-1}, respectively. The zeta potential of aggregates remained stable around -20 mV.

5.2.2 Zebrafish lines

Zebrafish were housed at Leiden University's zebrafish facility at 28 °C and with the photoperiod set to 14 h light:10 h dark. Husbandry and handling of the fish complied with Dutch national regulation on animal experimentation ('Wet op dierproeven' and 'Dierproevenbesluit 2014'), and European animal welfare regulations (EU Animal Protection Directive 2010/63/EU), as supervised by the Animal Welfare Body of Leiden University. Fish were bred and larvae were handled following the standard protocols included in 'The zebrafish book' (https://zfin.org).

Experiments were performed with larvae of AB×TL wildtype zebrafish, the transgenic reporter line *Tg(il1ß:eGFP-F)*, expressing farnesylated GFP under control of the *il1ß* promotor (Nguyen-Chi et al. 2014), and three loss-of-function mutants in the TLR2 signaling pathway. These mutants included a *tlr2-/-* mutant, a *myd88-/-* mutant and a *tirap-/-* mutant, comprising the *tlr2*^{sa19423} allele (ZFIN Cat# ZDB-ALT-131217-14694, RRID:ZFIN_ZDB-ALT-131217-14694), *myd88*^{hu3568} allele (ZFIN Cat# ZDB-ALT-130729-6, RRID:ZFIN_ZDB-ALT-130729-6) and *tirap*^{sa182} allele (ZFIN Cat# ZDB-ALT-100831-10, RRID:ZFIN_ZDB-ALT-100831-10), respectively. All mutant alleles were obtained in ENU mutation screens and comprised a threonine to alanine point mutation resulting in a pre-mature stop codon prior to (*tlr2*^{sa19423} and *myd88*^{hu3568}) or inside of (*tirap*^{sa182}) the TIR domain encoding sequence (Fig. 5.1b-d). The mutant alleles therefore encode truncated proteins without a functional TIR domain. All loss-of-function mutants and the transgenic line have an AB×TL background and have been approved by the Animal Welfare Body.

For the loss-of-function mutants, germ-free zebrafish larvae were obtained following 'Natural breeding method' described by Pham et al. (2008), with the modifications made by Koch et al. (2018). To this end, zebrafish eggs acquired from synchronized crosses were incubated for 6 h in egg water containing the antimycotic Amphothericin B (250 ng·mL^{-1}), and the antibiotics Ampicillin (100 µg·mL^{-1}) and Kanamycin (5 µg·mL^{-1}). Thereafter, 150 eggs were rinsed for 45 to 60 s with 3 mL 0.2% PVP-iodine solution in 15 mL conical tubes, and were subsequently rinsed twice with 10 mL autoclaved egg water. This procedure was followed by two rinsing steps of 5 min with 6 mL 0.03% sodium hypochlorite (3.5% Cl_2; VWR International, Radnor, PA).

Notably, this hypochlorite concentration is twice as low as the concentration used by Koch et al. (2018), to ensure that all embryos hatched naturally. In between hypochlorite rinsing steps, eggs were rinsed once with 10 mL autoclaved egg water. After the hypochlorite rinsing steps, eggs were rinsed thrice with 10 mL autoclaved egg water. Sterilized eggs were maintained in the dark under sterile conditions at 28 °C until the start of exposures at 3 days post-fertilization (dpf) (section 5.2.3). The sterility these 3-dpf larvae was checked by plating homogenized larvae on LB-medium, as described by Brinkmann et al. (2020).

5.2.3 Nanoparticle exposures

Zebrafish larvae were exposed to silver dispersions from 3-5 dpf. For exposures, the 24-well plate setup introduced by Van Pomeren et al. (2017b) was used. In this setup, ten larvae were exposed to 2 mL of exposure medium in one well of the 24-well plate. Larvae of controls were exposed to autoclaved egg water without nanoparticles. Three replicates were included per exposure concentration or control. Larvae in well plates were incubated in the dark at 28 °C, and mortality was scored at 0, 3, 7, 24 and 48 h post-exposure. At 24 h post-exposure, dead larvae were removed, and exposure media were refreshed.

Three different sets of exposures were tested, depending on the research question. Firstly, to study the accumulation of silver (section 5.2.4), AB×TL larvae were exposed to the lowest, sublethal nominal exposure concentration of 0.25 mg nAg·L^{-1}. Secondly, to study inflammatory responses (section 5.2.5), *Tg(il1ß:eGFP-F)* larvae were exposed to the sublethal nominal exposure concentration of 0.25 mg nAg·L^{-1}, and the corresponding shed ion concentration of 0.05 mg Ag^{+}·L^{-1}, as prepared from a $Ag(NO_3)$ stock solution. This enabled assessing the particle-specific inflammatory effects of nAg. Thirdly, to test the nAg-sensitivity of TLR2 signaling mutants (section 5.2.6.2), a full factorial exposure design, including each mutant and its sibling under both microbially-colonized and germ-free conditions, was applied for exposure to all nAg exposure concentrations.

5.2.4 Accumulation of silver in larvae and intestines

The uptake and adsorption of nAg by zebrafish larvae was determined by measuring total silver concentrations in larvae and their intestines. At 0, 7, 24 and 48 h post-exposure, larvae were sampled and anaesthetized with tricaine (200 µg·L^{-1}; 3-amino-benzoic acid; Sigma-Aldrich, Darmstadt, Germany). Intestines of anaesthetized larvae were extracted using two pairs of dissection tweezers, by pinching one pair of the tweezers in between the swim bladder and the intestines of the larvae, and gently pulling

the mid- and posterior intestine out of the tail of the larvae using the other pair of tweezers. Thereafter, the tissue covering the intestinal bulb was carefully removed, and intestines were cleaved at the basal side of the intestinal bulb. Intestines could not be collected at the start of exposures, as the intestinal tissue was still too fragile at this developmental stage. For three replicates at each exposure time, ten intestines were collected on one 2% agarose slice. Similarly, ten non-dissected larvae were collected on one 2% agarose slices at each exposure time *in triplo*. Agarose slices with intestines or larvae were transferred to pre-weighed 2.0 mL SafeLock microcentrifuge tubes (Eppendorf, Nijmegen, The Netherlands), and weighed again to determine the volume of agarose slices, which did not exceed 15 µL. Larvae and intestines were digested overnight at 70 °C in 200 µL 0.76× *aqua regia* (HNO_3 : HCl; 1 : 3), accounting for the volume of agarose slices. Digested samples were diluted to a final concentration of 2.25% HCl (1.06% HNO_3). Total silver in larval samples was measured by graphite furnace atomic absorption spectrometry (GFAAS; PinAAcle 900Z, Perkin Elmer, The Netherlands), and total silver in intestinal samples was measured by inductively coupled plasma mass spectrometry (ICP-MS; NexIon 2000, Perkin Elmer). Silver concentrations in larvae and their intestines were expressed as the total mass of Ag per larvae, and total mass of Ag per intestine, respectively.

5.2.5 Particle-specific inflammation

The pro-inflammatory effects of nAg were assessed using *Tg(il1ß:eGFP-F)* reporter larvae. At 48 h post-exposure, larvae of controls and larvae exposed to nAg (0.25 mg·L^{-1}) or Ag^+ (0.05 mg·L^{-1}) were transferred to a 0.5 % methylcellulose solution in egg water comprising the anesthetic tricaine (200 µg·L^{-1}). Anaesthetized larvae were laterally positioned on a 1% agarose plate for imaging using a stereo fluorescence microscope. Images were acquired of the green fluorescent signal, as detected using a GFP emission filter, and total transmitted light, as detected without emission filter. The sum of all pixel values in green fluorescence images was quantified from the posterior side of the swimbladder to the apical side of the tail using the 'RawIntDen' measurement in ImageJ (v. 2.0.0; Abràmoff et al. 2004). The area posterior of the swimbladder was excluded from the image analysis due to the high expression of GFP in the retina of control *Tg(il1ß:eGFP-F)* larvae (Nguyen-Chi et al. 2014). Ten larvae were imaged for each of the three replicates per treatment.

5.2.6 Statistical analysis

All statistical analyses were performed in R (v. 3.6.3; www.r-project.org), and all figures were plotted using Python (v. 3.6.5) with the packages 'numpy' (v. 1.19.1), 'pandas'

(v.0.23.3), and 'matplotlib' (v.3.1.3). Mean and standard error of the mean (SEM) are reported.

5.2.6.1 Il1ß expression of reporter larvae

The GFP signal of *Tg(il1ß:eGFP-F)* larvae was compared between control larvae, nAg-exposed larvae and Ag^{+}-exposed larvae by way of a one-way analysis of variance (ANOVA) combined with a Tukey's HSD post-hoc test. Logarithmic transformation was required to ensure that residuals followed a normal distribution, as assessed by inspecting histograms and Q-Q plots. Model residuals were plotted against fitted values to check for the equal distribution of variance across the treatments.

5.2.6.2 Sensitivity of TLR2 signaling mutants to nAg

The sensitivity of the TLR2 signaling mutants was compared to that of their wildtype siblings under germ-free and microbially colonized conditions by fitting time-response curves to mortality data using generalized linear mixed models. These models were fitted using the *glmer* function of the 'lme4' package (v. 1.1-23), for all five exposure concentrations, excluding controls. All models included the 'dead' or 'live' state of larvae as binary response variable, and exposure time, exposure concentration, genotype ('mutant' vs. 'wildtype') and colonization condition ('colonized' or 'germ-free') as explanatory variables. Significant interactions between these four explanatory variables, as indicated in Table 5.1, were also included in the models. Additionally, exposure well was included as random variable in all models, to account for the repeated scoring of mortality over time for these wells. The *logit* link function was used to specify the binomial family of the generalized linear mixed models. Moreover, a *bobyqa* optimizer function with 2^5 iterations was applied for TLR2 and TIRAP models to solve convergence failure. To plot the fitted time-response curves, predicted probabilities were obtained from mixed models using the *predict* function.

To check model assumptions, Q-Q plots were computed using the 'car' package (v. 3.0-8), to examine if model residuals followed a normally distributed. Furthermore, Pearson model residuals were plotted against fitted values, to verify the equal spread of variance across the treatments. Theta values of the mixed effect were extracted to check for potential singularity. In case none of these assumptions were violated, post-hoc comparisons were performed using the *glth* function of the 'multcomp' package (v.1.4-13) in four consecutive steps. Firstly, we tested if microbiota indeed offered protection against nAg, by comparing the nAg-sensitivity of wildtype siblings under germ-free and

Table 5.1: Significant interactions included in dose-response models.

	Model		
Interactions	*TLR2*	*MyD88*	*TIRAP*
Hours : Condition	x	x	x
Hours : Genotype	x		
Hours : Concentration	x	x	
Genotype : Condition			x
Genotype : Concentration			x
Hours : Genotype : Condition	x		x
Hours : Genotype : Concentration			x

microbially-colonized conditions. Secondly, we tested if this protective effect was lost in the loss-of-function mutants, by comparing the nAg-sensitivity of TLR2 signaling mutants under germ-free and microbially colonized condition. Thirdly, we examined if there were any microbiota-independent effects of TLR2 signaling on nAg-sensitivity, by comparing the nAg-sensitivity of TLR2 signaling mutants and wildtype siblings under germ-free conditions. Fourthly, in case no microbiota-independent effects could be detected, we evaluated if the level of protection against nAg offered by colonizing microbiota was affected in TLR2 signaling mutants, by comparing the nAg-sensitivity of TLR2 signaling mutants and their wildtype siblings under microbially colonized conditions.

5.3 Results

5.3.1 Accumulation of silver in total and intestinal tissues

Zebrafish larvae gradually accumulated silver in and on their tissues over the two-day exposure to sublethal concentrations of nAg (0.25 mg nAg·L^{-1}) (Fig. 5.2). The concentration of silver associated with the total larval tissue increased linearly over time, reaching a final concentration of 0.29 ± 0.01 ng Ag·$larva^{-1}$ at the end of exposure (Fig. 5.2, black circles). Less than 10% of this total amount of tissue-associated silver accumulated in the intestines of larvae (Fig. 5.2, white circles). Most of this silver accumulated in the intestines over the first day of exposure, reaching an average concentration of 0.008 ± 0.0003 ng Ag·$intestine^{-1}$ at 24 h of exposure. Over the second exposure day, only a slight increase to 0.011 ± 0.0009 Ag·$intestine^{-1}$ was detected, indicating a saturation of the intestinal exposure to nAg.

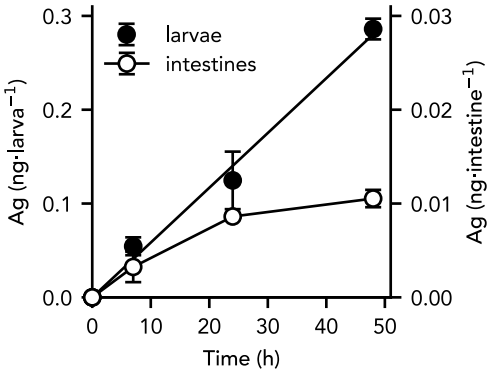

Figure 5.2: *Accumulation of total silver in zebrafish larvae*. Black circles (left axis) represent silver concentrations in and on the entire larvae, white circles (right axis) represent silver concentrations in the intestines of larvae.

5.3.2 Particle-specific inflammation induced by silver nanoparticles

The intensity and localization of pro-inflammatory effects of nAg were assessed based on the expression of the pro-inflammatory cytokine encoding gene *il1ß* in transgenic *Tg(il1ß:eGFP-F)* reporter larvae. Following two days of exposure, sublethal concentrations of nAg (0.25 mg·L^{-1}) resulted in enhanced expression of *il1ß* in patches along the complete surface of the skin of zebrafish larvae (Fig. 5.3a). At some of these patches, tissue damage could clearly be observed using stereo microscopy. The total *il1ß* signal, as quantified by the log-transformed integrated density of GFP signal in microscopy images, was significantly higher in nAg-exposed larvae (14.38 ± 0.07) than in control larvae (13.82 ± 0.03) ($p < 0.001$). No tissues with enhanced *il1ß* expression could be observed in larvae that were exposed to silver ions at concentrations that correspond to the dissolved fraction of nAg in particle exposures (0.05 mg Ag^{+}·L^{-1}) (Fig. 5.3b). Similarly, no indications of an enhanced *il1ß* signal could be observed in controls that had not been exposed to silver ions and particles (Fig. 5.3c). Accordingly, the total *il1ß* signal in Ag^{+}-exposed larvae (13.92 ± 0.05) and controls (13.82 ± 0.03) did not differ significantly ($p = 0.42$).

5.3.3 Microbiota-dependent sensitivity of TLR2 signaling mutants to silver nanoparticle toxicity

To gain further mechanistic understanding of the protective effect of microbiota against the adverse effects of nAg, resulting from aquatic exposure as characterized above, we compared the sensitivity of three loss-of-function mutants in the TLR2 signaling pathway in acute toxicity tests. We specifically focused on mutants for TLR2 (Fig. 5.4), and TLR2 adaptor proteins MyD88 and TIRAP (Fig. 5.5). To allow detecting subtle

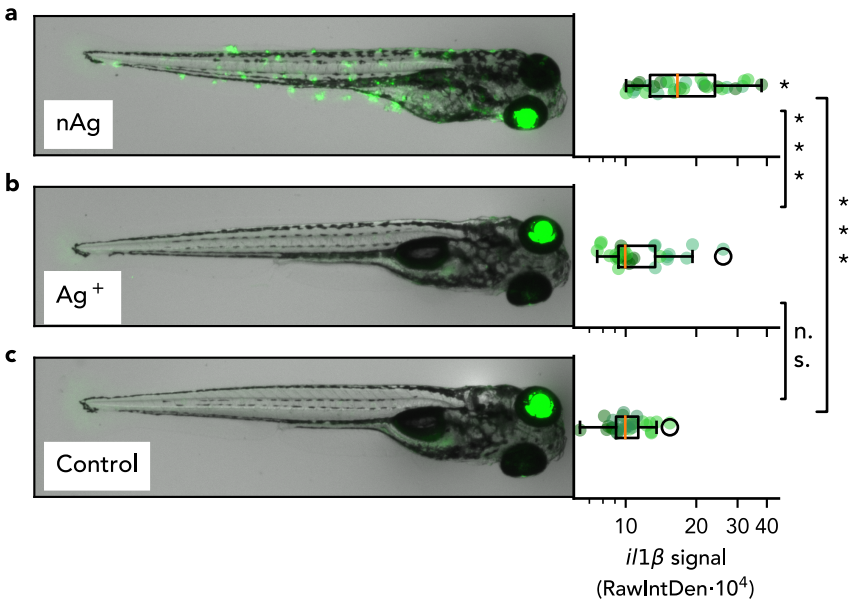

Figure 5.3: *Particle-specific inflammatory effect of silver nanoparticle exposures.* Inflammatory effects were studied using *Tg(il1ß:eGFP-F)* reporter zebrafish larvae. Pictures show representative images of larvae, with quantification of GFP signal from the anterior side of the swim bladder up to and including the tail fin, following exposure to nAg (0.25 mg nAg·L^{-1}; *n*=30) (**a**), their shed ions (0.05 mg Ag^{+}·L^{-1}; *n*=30) (**b**), and egg water lacking nAg and shed ions (*n*=28) (**c**). Asterisks indicate significant differences: ***, $p<0.001$. *Abbreviations*: RawIntDent, Raw integrated density; n.s., non-significant.

differences in the protective effects of microbiota between the TLR2 signaling mutants, time response curves for the full range of exposure concentrations were used in all acute toxicity comparisons.

Before we evaluated the effects of microbial interactions with the TLR2, MyD88 and TIRAP proteins on nAg toxicity to zebrafish larvae, we first checked if the genetic background of these mutants affected nAg sensitivity. For siblings of all mutants, microbially-colonized larvae were less sensitive to nAg than germ-free larvae (TLR2: $p < 0.001$, $z = -8.21$; MyD88: $p < 0.001$, $z = -9.83$; TIRAP: $p < 0.001$, $z = -8.92$). The mortality of nAg-exposed siblings followed similar time-response patterns, where the difference in mortality between germ-free and colonized conditions was largest at the start of exposure and decreased gradually over time (Fig. 5.4 and Fig. 5.5, black curves). These results indicate that, irrespective of genetic background, colonizing microbiota protected zebrafish larvae against nAg toxicity, while this protective effect dissipated over time. We subsequently examined if there were any microbiota-independent effects of the loss-of-function mutations on nAg toxicity. Since, under germ-free conditions,

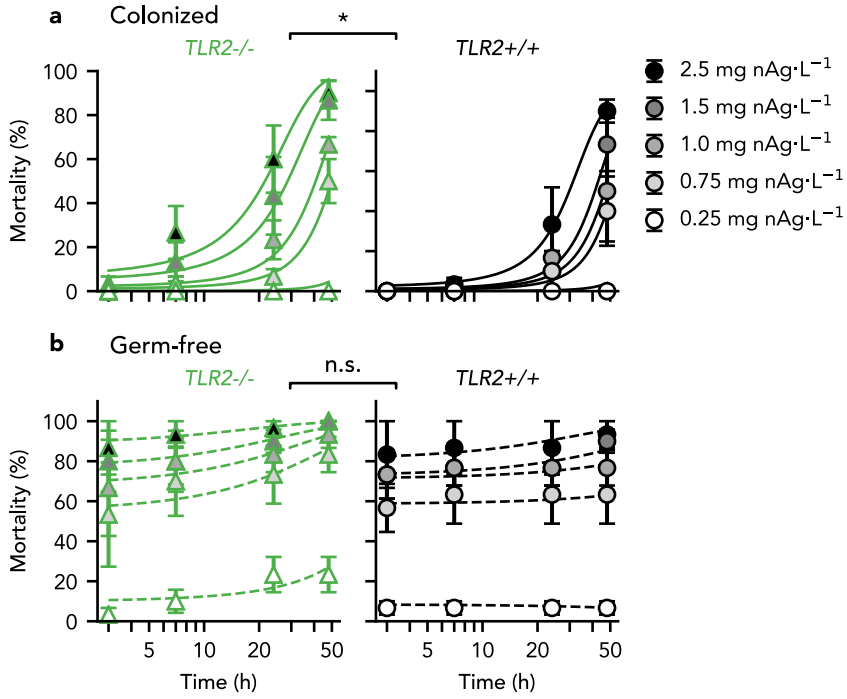

Figure 5.4: *TLR2-dependent effects of colonizing microbiota on silver nanoparticle toxicity to zebrafish larvae*. Sensitivity of *tlr2*$^{-/-}$ as compared to *tlr2*$^{+/+}$ zebrafish larvae under microbially-colonized conditions (**a**) and germ-free conditions (**b**). Asterisks indicate significant differences (*n=3*).

the nAg-sensitivity of all mutants did not differ from that of their wildtype siblings (TLR2: $p = 0.90$, $z = -0.12$; MyD88: $p = 0.73$, $z = 0.35$; TIRAP: $p = 0.14$, $z = -1.49$) (Fig. 5.4b, Fig. 5.5c,d), these effects could not be detected.

The lack of microbiota-independent effects on nAg-sensitivity for all mutant lines allowed us to explore to what extent microbiota-dependent effects on nAg-sensitivity involve signaling through TLR2, MyD88 or TIRAP. All loss-of-function mutants were less sensitive to nAg under microbially-colonized conditions than under germ-free conditions (TLR2: $p < 0.001$, $z = -7.14$; MyD88: $p < 0.001$, $z = -9.23$; TIRAP: $p < 0.001$, $z = -8.08$), indicating that the protective effect of microbiota against nAg was maintained in the absence of functional TLR2, MyD88 or TIRAP protein. Nevertheless, the level of protection offered by colonized microbiota against nAg toxicity depended on the loss-of-function mutations. Under microbially-colonized conditions, *tlr2* mutants were more sensitive to nAg than their wildtype siblings ($p = 0.04$, $z = 2.01$) (Fig. 5.4a). Similarly, *tirap* mutants were more sensitive to nAg under microbially-colonized conditions than wildtype siblings ($p < 0.001$, $z = 4.51$) (Fig. 5.5b). This implies that

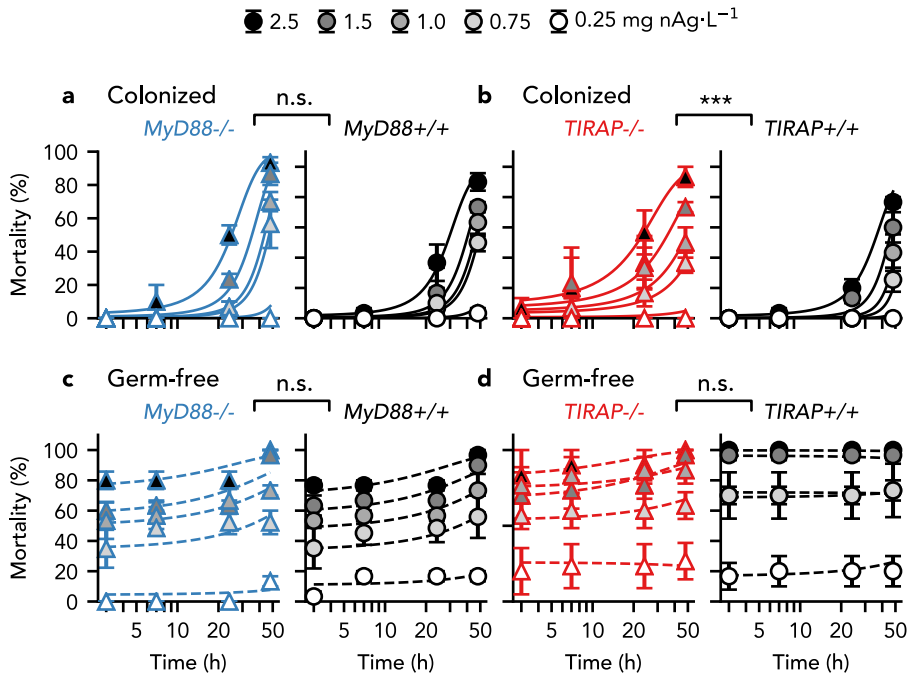

Figure 5.5: *TLR2 adaptor-dependent effects of colonizing microbiota on silver nanoparticle toxicity to zebrafish larvae*. **a**) and **c**) Sensitivity of *myd88*$^{-/-}$ as compared to *myd88*$^{+/+}$ zebrafish larvae, under microbially-colonized conditions (**a**) and germ-free conditions (**c**). **b**) and **d**) Sensitivity of *tirap*$^{-/-}$ as compared to *tirap*$^{+/+}$ zebrafish larvae, under microbially-colonized conditions (**b**) and germ-free conditions (**d**). Asterisks indicate significant differences (n=3).

microbial interactions with TLR2 affect the sensitivity of zebrafish larvae to nAg in a TIRAP-dependent manner. In contrast to *tlr2* and *tirap* mutants, the sensitivity of the *myd88* mutant did not differ significantly from that of wildtype siblings under microbially-colonized conditions (p = 0.52, z = 0.47) (Fig. 5.5a).

5.4 Discussion

Studies investigating the role of host-microbiota interactions in nanomaterial toxicity face the common challenge to differentiate between the direct effects of microbe-particle interactions on the fate, behavior and reactivity of nanoparticles (Lowry et al. 2012), and the effects of host-microbiota interactions on the host's sensitivity to particle toxicity. In diverse animals, with most evidence provided for vertebrates (Dierking and Pita 2020), interactions between commensal microbiota and the host have been shown to depend on the recognition of microbial constituents by receptors of the TLR family. Here, we explored if we could identify impacts of host-microbiota interactions on

nanomaterial toxicity based on TLR2 signaling. To this end, we focused on the protective effect of colonizing microbiota against nAg toxicity to zebrafish larvae, employing the experimental benefits and available mutant lines for this widely used model organism.

The first step towards understanding the protective effects of colonizing microbiota against nAg toxicity, was to characterize the actual exposure to nAg over time, as well as to quantify and localize the adverse effects that this imposes on the larvae. Briefly, we found that silver accumulated gradually in and on the larval bodies from the start of exposure onwards, with a small fraction reaching the intestines. This intestinal silver exposure accounted less than 10% of the total body burden. In contrast to the total body burden, the accumulation of silver in intestines saturated over time. It is plausible that this saturation resulted from the impaired swallowing activity of larvae that have been affected by the pro-inflammatory effects of nAg.

To characterize these pro-inflammatory effects of nAg, we used fluorescent reporter larvae expressing GFP under control of the *il1ß* promotor. Imaging of these larvae showed that nAg exposure resulted in enhanced *il1ß* expression in patches across the full skin of larvae. The transcriptional investigations of Kang et al. (2016), showing a >2-fold higher expression of *il1ß* (BC098597 / NM_212844) by zebrafish larvae that were exposed to a sublethal concentration of nAg, as compared to control larvae, corroborate this finding. Because we also observed tissue damage at these locations with enhanced *il1ß* expression, the pre-cytokine had likely been activated by pyrin containing protein-3 (NLRP3) and caspase-1 (Dinarello 2018). Notably, these pro-inflammatory effects could not be detected in zebrafish larvae that had been exposed to silver ions at concentrations corresponding to the dissolved fraction of the particle exposures. Although the applied analytical techniques do not allow for the quantification of silver in dermal versus internal tissues, and can neither discriminate between the particulate and dissolved fractions of silver, these particle-specific adverse effects suggest that nAg adsorbed onto the skin of zebrafish larvae, causing local dermal inflammation. Similar dermal pro-inflammatory effects of nanoparticles have previously been described by Brun et al. (2018) for both copper and plastic nanoparticles.

Although the *il1ß* reporter larvae allow to detect pro-inflammatory cytokine responses in internal tissues (Nguyen-Chi et al. 2014), we only detected increased *il1ß* expression on the skin of larvae. Previous research on the adverse effects of nAg to zebrafish larvae revealed that ionocytes, a skin cell type, and sensory systems, including the olfactory bulb and neuromasts, are particularly sensitive to nAg-induced oxidative stress, showing responses at concentrations from 4 $\mu g \cdot L^{-1}$ to 1 mg $nAg \cdot L^{-1}$ (Osborne et al. 2016; Horng et al. 2022). At higher exposure concentrations, starting at 1 mg $nAg \cdot L^{-1}$, oxidative stress could also be observed in the intestines of zebrafish larvae (Liu et al.

2019; Lee et al. 2022). In nanomaterial toxicity, levels of oxidative stress that cannot be compensated via the regulation of cytoprotective (antioxidant) genes ('tier 1' oxidative stress) are hypothesized to result in inflammatory responses ('tier 2' oxidative stress), and eventually, if ROS levels increase even further, in cytotoxic and genotoxic responses ('tier 3' oxidative stress) (Johnston et al. 2018). Since both neuromasts and ionocytes are located on the skin of zebrafish larvae, it is possible that the dermal inflammation observed in our study originates from nAg-induced oxidative stress in these sensory systems and cells.

Next, to study the protective effect of microbiota against nAg, we compared the lethal effects of nAg between larvae raised under microbially-colonized and germ-free conditions. The difference in mortality between these conditions can be attributed to the protective effect of colonizing microbiota against nAg toxicity to zebrafish larvae. In the absence of microbiota, nAg induced high and nearly instant mortality at concentrations that were only lethal to microbially-colonized larvae by the second day of exposure. Such nearly instant mortality has been associated with septic shock, which can be induced by exposing zebrafish larvae to immunostimulants such as lipopolysaccharides (Philip et al. 2017). Similar to the protective effect of microbiota against acute nAg-induced mortality, synbiotics comprising commensal microbes have been reported to protect early infants against sepsis (Panigrahi et al. 2017). These remarkable commonalities could indicate that nAg toxicity and sepsis involve similar hyperinflammatory states.

In our study, we showed that a loss-of-function mutation in TLR2 limits the protective effect of colonizing microbiota against nAg toxicity to zebrafish larvae. This indicates that microbial interactions with TLR2 confer protection against nAg toxicity to zebrafish larvae. Crucially, under germ-free conditions we could not detect any difference in sensitivity between *tlr2* mutants and their wildtype siblings. This supports two important assumptions that are inherent to our experimental setup. It firstly suggests that interactions of colonizing microbiota with TLR2, rather than interactions of sterile TLR2 agonists, such as damage-associated molecular patterns (DAMPs) that are released upon wounding, affect nAg toxicity to zebrafish larvae. It secondly shows that differences in sensitivity between mutants and their siblings do not result from direct effects of nAg on TLR2 signaling. This is an important assumption to validate, as nAg has previously been found to affect lipopolysaccharide-induced TLR signaling in THP-1 cells (Gliga et al. 2019).

Downstream signaling from TLR2 requires the intracellular recruitment of TLR2 adaptor proteins TIRAP and MyD88. Together with interleukin 1 receptor (IL-1R) associated kinase 4 (IRAK-4), and IRAK-1 or IRAK-2, these adaptor proteins form a protein complex called the 'Myddosome', which transduces the TLR2 signal

intracellularly (Lin et al. 2010). In view of this signaling cascade, reproducing the results obtained for the *tlr2* mutant in loss-of-function mutants for TIRAP or MyD88 could provide further support for the hypothesis that colonizing microbiota protect zebrafish larvae against nAg toxicity via signaling through TLR2. However, only the loss-of-function mutant for TIRAP, but not the loss-of-function mutant for MyD88, could reproduce the higher microbiota-dependent sensitivity to nAg toxicity observed for the *tlr2* mutant. This discrepancy could indicate that the protective effect of colonizing microbiota against nAg toxicity involves MyD88-independent TLR2 signaling pathways, as have been described by Bernard and O'Neill (2013) and Rajpoot et al. (2021). Alternatively, the contrasting results for MyD88 and TIRAP could reflect the more complex role of MyD88 in intracellular signaling. While, to our current understanding, TIRAP is only involved in signaling from TLR2 and TLR4, and in signaling from the receptor for advanced glycation end-products (RAGE), MyD88 interacts with intracellular signaling pathways from all TLRs except for TLR3, and moreover interacts with the interleukin receptors IL-1R and IL-18R (Adachi et al. 1998), as well as RAGE (Rajpoot et al. 2021) and IFN-γR (Sun and Ding 2006). Potentially, the effects of the loss-of-function mutation for MyD88 on signaling from these receptors could mask its effects on TLR2 signaling. Despite the complexity in these signaling pathways, the finding that loss-of-function mutations in two key proteins of the TLR2 signaling pathway result in higher, microbiota-dependent sensitivity of zebrafish larvae against nAg toxicity, strengthens the support for the identified role of TLR2 signaling in the protective effect of colonizing microbiota against nAg toxicity.

The observed responses of zebrafish larvae to nAg, including protective TLR2 signaling and enhanced *il1ß* expression, could be part of a pathophysiological manifestation initiated by particle-induced oxidative stress, and resulting in tissue damage. Here, the elevated *il1ß* expression can be an indication of the inflammatory response to 'tier 2' oxidative stress, in which neutrophils and macrophages infiltrate the particle-exposed tissue (Johnston et al. 2018). The enhanced *il1ß* expression by epithelial cells can also stimulate the regeneration of injured tissue via the expression of regenerative genes (Hasegawa et al. 2017). Similarly, microbiota-induced TLR2 expression can promote cell proliferation via ERK and AKT signaling (Hörmann et al. 2014). This is consistent with the expression study of Kang et al. (2016), showing that not only the expression of *il1ß*, but also the expression of genes from the TLR, MAPK/ERK and cell cycle pathways were upregulated in response to nAg. Nevertheless, if inflammatory cytokines and immune cells are not cleared from the target site, chronic inflammation can result in cytotoxicity, genotoxicity (Johnston et al. 2018) and apoptosis of regenerative cells (Hasegawa et al. 2017).

Irrespective of what intracellular signaling pathways confer the protective effect of

colonizing microbiota against nAg toxicity to zebrafish larvae, only a small fraction of the mortality that could be prevented by microbial colonization was TLR2-dependent. Part of the remaining mortality that is specific to the germ-free condition may be attributed to the lack of host-microbiota interactions through other receptors. In fact, adult zebrafish express at least seventeen putative TLR variants, including counterparts for human TLRs (TLR-1,-2,-3,-4,-5,-7,-8,-9), several non-mammalian TLRs (TLR-18, -19, -20, -21, and -22), and variants resulting from the genome duplication event in teleost fish (tlr4ba/tlr4bb for TLR-4; tlr5a/tlr5b for TLR-5; tlr8a/tlr8b for TLR-8; tlr20a/trl20b for TLR-20) (Meijer et al. 2004; Li et al. 2017). Additionally, direct interactions between microbes and nanoparticles would be expected to alter nAg toxicity to zebrafish larvae by affecting particle fate, biodistribution and reactivity (Lowry et al. 2012; Westmeier et al. 2018). Intuitive examples of such interactions include the enhanced aggregation of nAg in the presence of microbial exudates like flagellin (Panáček et al. 2018), as well as the reduction of toxic silver ions by microbial activity (Lin et al. 2014). It is beyond the scope of the present work to assess the relative contributions of these microbe-particle interactions, compared to the effects of host-microbiota interactions on nanomaterial toxicity. Nonetheless, for the first time, our study provides evidence that the recognition of colonizing microbiota by TLR2 affects nanomaterial toxicity *in vivo*. This demonstrates the importance of considering the intricate interactions between hosts and their microbiota in nanomaterial hazard assessment.

5.5 Conclusions

In this study, we show that suspended nAg can accumulate on the skin of zebrafish larvae, causing particle-specific dermal inflammation at sublethal exposure concentrations. At lethal exposure concentrations, nAg induced more acute mortality patterns under germ-free conditions than under microbially-colonized conditions. The nearly instant mortality under germ-free conditions could potentially result from hyperinflammatory states that have been described for septic shock. We found that colonizing microbiota can protect against this nAg-toxicity in a partly TLR2- and TIRAP-dependent manner. Since TLR2 and TIRAP are key proteins of the TLR2 signaling pathway, this reveals that microbiota-host interactions can shape the response of the host to immuno-toxic nanoparticles. This confirms the importance of including the role of host-microbiota interactions in nanoparticle effect assessment.

Author contributions

Bregje W. Brinkmann: Conceptualization, Investigation, Formal analysis, Writing – original draft, Writing – review & editing. ***Bjørn E.V. Koch***: Conceptualization, Writing – review & editing. ***Willie J.G.M. Peijnenburg***: Supervision, Writing – review & editing. ***Martina G. Vijver***: Supervision, Funding acquisition, Writing – review & editing.

Data availability statement

Data is available via Mendeley Data DOI: 10.17632/4nfg69v8hy.1

Acknowledgments

The authors are grateful to Rudo Verweij for his support with GFAAS measurements, Sipeng Zheng for performing ICP-MS measurements, Wouter Beijk for help with stereo fluorescence imaging, Wanbin Hu for help with maintenance and genotyping of the mutant zebrafish lines, Mónica Varela for maintaining the *il1ß*-reporter zebrafish, Annemarie Meijer for providing the *myd88-/-* mutant, Herman Spaink for providing the *tlr2-/-* mutant, as well as for his valuable input in scientific discussions, and the anonymous reviewer for providing constructive comments. The authors thank HeiQ RAS AG for providing silver nanoparticles for this study. This work was supported by the project PATROLS of European Union's Horizon 2020 research and innovation programme [grant number 760813].